Polarimetric measurements of long-wave infrared spectral radiance from water

Joseph A. Shaw

Polarimetric measurements of the thermal infrared spectral radiance from water are reported and are compared with calculations from a recently published model over the spectral range of 600–1600 cm^{-1} (6.25–16.67-μm wavelength). In this spectral range, warm water viewed under a dry, clear atmosphere appears vertically polarized by 6–12%. The measured spectral degree of polarization agrees with calculations within the measurement uncertainty (~0.5% polarization in spectral regions with high atmospheric transmittance and 1.5% polarization in spectral regions with low atmospheric transmittance). Uncertainty also arises from temporal changes in water and air temperatures between measurements at orthogonal polarization states, indicating the desirability of simultaneous measurements for both polarization states.

OCIS codes: 010.0010, 120.5410, 120.5630, 120.0280, 120.0120.

1. Introduction

In a previous publication I described model results of the spectral degree of polarization for thermal infrared radiance from water over the spectral band of 3–15 μm.[1] I used this computer model to show how each component of the total radiance affects the final polarization state. Key results of this analysis were (1) long-wave infrared water radiance is almost always vertically polarized, whereas shortwave (wavelength $\lesssim$ 3.4 μm) radiance tends to be horizontally polarized during the day because of reflected skylight (shortwave infrared radiance can be vertically polarized at night); (2) the degree of polarization depends strongly on the radiometric contrast between the water emission and the background reflection; and (3) Sun glints covering more than approximately 0.3% of the observed scene area cause the entire spectrum to be horizontally polarized. A consequence of the second point, regarding radiometric contrast, is that water viewed under a clear sky appears more vertically polarized than the same water viewed under a cloudy sky.

Thermal infrared emission is partially polarized in the vertical plane when a horizontally oriented emitting surface is viewed obliquely.[1–4] As the viewing angle increases from normal, the degree of emission polarization increases from zero to a maximum determined by the index of refraction of the material and the viewing angle. This kind of thermal emission polarization exists for all surfaces that are not ideal blackbodies. Millikan,[3] in 1895, originally proposed that emission polarization should be treated as arising from refraction of otherwise unpolarized radiation as it transmits across the interface between the material and the air. This explanation was repeated and amplifed in a pioneering review article by Sandus in 1965.[4] Thus emission polarization can be calculated when the unpolarized blackbody radiation is multiplied by the Fresnel transmissivity for the appropriate interface between two media. Emission polarization also can be calculated when the the surface reflectivity is subtracted from one, if the emitting medium has no net transmission such that the sum of reflectivity and emissivity is equal to one.

The complementary nature of emission and reflection can be useful when we think about emission polarization in the often more familiar terms of reflection polarization. As the viewing angle increases toward the Brewster angle for a horizontal surface, the vertically polarized component of emissivity increases and the horizontally polarized component decreases, relative to the normal-incidence value. At

When this research was performed, the author was with the National Oceanic and Atmospheric Administration Environmental Technology Laboratory, 325 Broadway, Boulder, Colorado 80305-3328. He (jshaw@ece.montana.edu) is now with the Department of Electrical and Computer Engineering, Montana State University, Bozeman, Montana 59717.

Received 7 December 2000; revised manuscript received 5 July 2001.

0003-6935/01/335985-06$15.00/0

the Brewster angle the vertically polarized emissivity approaches unity, reaching unity if the surface is lossless. Beyond the Brewster angle, both emissivity components fall below the normal value, always with the vertical component larger than the horizontal component. This is all just the opposite of the familiar polarization of reflected light, for which the vertically polarized component of reflectivity approaches zero at the Brewster angle, leaving horizontally polarized light.

A unique characteristic of emission polarization is that the degree of polarization magnitude increases monotonically with angle. The maximum surface-emission vertical polarization occurs at 90° and is typically 20–30% for water in the thermal infrared spectral range. By contrast, the horizontal polarization of reflected light increases with angle up to a maximum at the Brewster angle (typically ~48°–56° for water in the thermal infrared region) and then decreases again to zero at 90°.

The polarization state of radiance that is actually observed from water arises from a combination of surface emission and background reflection. The water emission is vertically polarized, whereas the background reflection is horizontally polarized, so the net polarization depends strongly on the radiometric contrast between the water and the reflected background. Even for a radiometrically cool background atmosphere (e.g., clear skies with low water vapor), the reflected-background polarization eventually overwhelms the surface-emission polarization at very large viewing angles (usually above approximately 80°) where the surface reflection rapidly increases toward 100%. This angular behavior of polarization for broadband, spectrally integrated water radiance was verified previously.[1]

The previous measurements to verify the water polarization computer model were limited to data from a filter radiometer covering the long-wavelength band of 9.9–11.5 μm (870–1010 cm^{-1}) in a single spectral channel.[1] Therefore the purpose of this paper is to present the first comparison of model results with spectrally resolved measurements. This comparison is for measurements of the spectral degree of polarization in the long-wave atmospheric window spectral region of 600–1600 cm^{-1} (6.25–16.67-μm wavelength). These new measurements were made with a Fourier transform infrared (FTIR) spectroradiometer with a wire-grid infrared polarizer at the entrance port.

The measurements presented here contribute useful validation of the computer model, but also illustrate needed improvements in polarization measurements and in the environmental characterization that serves as the model input. This study and future research will improve understanding of infrared polarization of natural scenes, benefiting both environmental[1,2] and military[5–7] remote sensing.

2. Spectral Polarization Measurements

Spectrally resolved polarized emission measurements were provided by a FTIR spectroradiometer with a wire-grid polarizer in a rotating mount replacing the ZnSe emission port window. The polarizer grid, on a ZnSe substrate, has a specification of better than 1:200 extinction ratio in the spectral region considered here. The FTIR signal is recorded with a HgCdTe detector operating at 77 K. With the instrument looking at water, spectra were calibrated with measurements of two blackbody calibration sources operating at temperatures of 20 °C and 60 °C in the same manner that is used routinely with this instrument to measure atmospheric emission.[8,9] Total elapsed time between calibrations varied between 5 and 15 min, which our experience in many field deployments has shown to produce radiometric uncertainty less than 1% of ambient blackbody radiance in measurements of atmospheric emission with 30 coadded scans at each target (cold blackbody, warm blackbody, and the atmosphere).[8,9] For these water polarization measurements, separate sequences of water and calibration source spectra were recorded at horizontal and vertical polarization.

The spectrometer (Bomem MR100) and blackbody calibration sources used in this experiment are the same ones we use for atmospheric emission measurements, with the only significant difference being replacement of the ZnSe emission port window with a wire-grid polarizer. The calibration sources are thermoelectrically controlled honeycomb surfaces, which provide long-wave infrared emissivity of approximately 0.996. For atmospheric measurements, the spectrometer emission port views a gold beam-steering mirror, which a stepper motor turns to alternately direct the beam into the two calibration sources and the atmosphere. For the water polarization measurements, the spectrometer was mounted on a tilted plate to view the water surface, and the calibration sources were held directly in front of the spectrometer's emission port.

The beam splitter and mirrors in the interferometer cause FTIR spectrometers to almost always have a significant variation of instrument response with polarization. Our particular FTIR instrument is approximately 6% more sensitive to vertically polarized radiance than to horizontally polarized radiance over a 700–1650-cm^{-1} spectral range.[10] However, performing separate calibrations at each polarizer setting compensates for this instrument polarization response. In fact, measuring the degree of polarization of a source does not require radiometric calibration if the instrument response does not change with polarization.

Measuring the thermal infrared polarization signature of water requires a radiometrically cold background, or else the vertical emission polarization component is effectively cancelled by the horizontal reflection polarization component from a bright background. Therefore such measurements are best made outside under a radiometrically cold clear sky. To achieve some of the protection and stability of a laboratory while still providing a clear-sky background, I made the measurements reported here in a rooftop laboratory with the instrument pointed such

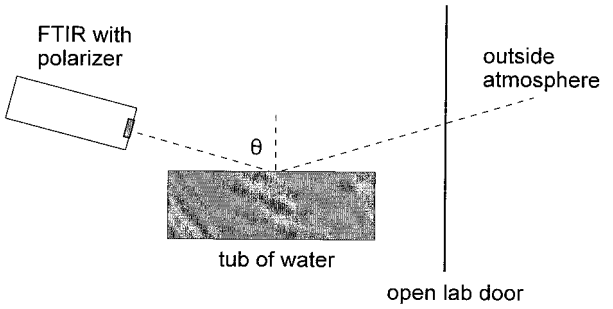

Fig. 1. Layout of the infrared water polarization measurement experiment. The FTIR spectroradiometer, calibration sources (not shown), and tub of water were inside a laboratory with an open door so that the reflected background was the clear outside atmosphere.

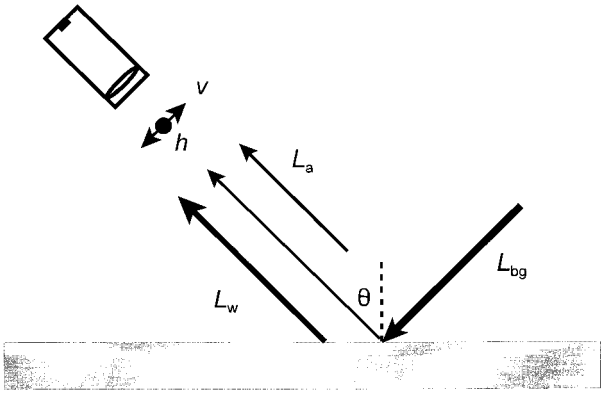

Fig. 2. Components and geometry for the polarimetric radiative transfer program used to calculate infrared water polarization.

that the background reflection came from the clear sky seen through open doors. As indicated in Fig. 1, the FTIR instrument was pointed at a tub of water with incidence angle $\theta = 75°$ (with respect to the surface normal) to maximize the expected degree of polarization. The distance from the FTIR emission port to the water was approximately 0.7 m, and the distance from the water to the air outside the laboratory was approximately 1 m; beyond that was outside air with a surface temperature of 0 °C and a cloud-free sky. Profiles of atmospheric temperature, humidity, and gas concentration measured at the same time as the water spectra could have helped to better characterize the background in the model. The bulk water temperature was 47 °C at the start of the measurements and 31 °C at the end, and the air temperature near the water (inside the laboratory) varied between 13 and 20 °C, depending on whether the laboratory doors were open or closed. Temperatures were recorded before and after each measurement sequence.

For the results shown here, the time required to record spectra for the water and the two calibration sources was approximately 5 min for each polarization state, during which ten spectra at each target were averaged to reduce noise. In spectral regions with moderately strong atmospheric absorption (primarily from carbon dioxide and water vapor), it was challenging to keep large errors from occurring because of changing air temperature and humidity as the laboratory doors were opened and closed during the measurement period. However, the measurements are shown only for a spectral range where these errors were most consistently avoided during several weeks when I experimented with different approaches to using this FTIR instrument to measure both water polarization and instrument polarization sensitivity.

From the calibrated water spectra at each polarizer setting, the spectral degree of polarization is calculated as

$$\mathrm{DP}(f) = \frac{L^h(f) - L^v(f)}{L^h(f) + L^v(f)}, \qquad (1)$$

where $L(f)$ is the spectral radiance [W/(m^2 sr cm^{-1})] at wave number f (cm^{-1}), and the superscripts indicate either horizontal (h) or vertical (v) polarization. The magnitude of DP(f) tells how strongly polarized the light is, and the sign tells its polarization direction (positive for h polarization and negative for v polarization). In multiple repetitions of the measurements for both polarizations, the degree of polarization had an uncertainty of approximately 0.002–0.01 (0.2–1% polarization) in spectral regions of high atmospheric transmittance and 0.01–0.03 (1% and 3% polarization) in spectral regions of low atmospheric transmittance.

3. Spectral Polarization Calculations

In this section I provide a brief description of the computer model used to calculate the infrared spectral degree of polarization for water. A previous publication provides a more detailed description of this model and the results from it being used to study the polarization signature of water over the thermal infrared wavelength range of 3–15 μm for a variety of meteorological conditions, instrument heights, and incidence angles.[1] The model computes polarization spectra for different conditions of atmospheric emission, atmospheric transmission, and water refractive index. The atmospheric transmission and emission are calculated with the MODTRAN3 radiative transfer program[11,12] and the water refractive index is based on the compilation of Hale and Querry.[13]

The polarimetric radiative transfer model combines the radiative components illustrated in Fig. 2 to compute the total radiance from a horizontal water surface measured at horizontal h and vertical v linear polarization states at a viewing angle of θ. The net spectral radiance [W/(m^2 sr cm^{-1})] contains emission from the water surface (L_w) and the atmosphere between the sensor and the water (L_a), in addition to reflected background emission (L_{bg}). The water surface is modeled as a specular surface with an optional rough surface[14] consisting of specular facets with a wave-slope distribution given by the isotropic Gaussian term of the Cox–Munk model[15] (without the sometimes important higher-order slope statistics

terms, but with the option of using the Shaw–Churnside correction for stability dependence of the mean-square slope[16]).

The specular-path background radiance becomes partially polarized upon reflection from the water surface according to the reflectivity $R_w^{h,v}$, and both the reflected background radiance and the surface-emitted radiance are attenuated by the atmospheric transmittance τ_a. The combination of these elements, each of which is a function of angle θ and spectral wave number f, produces the net radiance in each polarization state (indicated by superscripts h and v) according to

$$L^{h,v} = \tau_a(L_w^{h,v} + R_w^{h,v}L_{\mathrm{bg}}) + L_a. \quad (2)$$

From the two polarization components of total radiance [Eq. (2)], the degree of polarization DP is calculated according to Eq. (1).

In Eq. (2) the atmospheric transmittance and emitted radiance terms are calculated at each spectral bin with MODTRAN3. Emission from the water surface is calculated as blackbody radiance at the water-surface temperature, multiplied by the water emissivity ϵ_w, which is calculated as one minus the water reflectivity R_w,

$$\epsilon_w^{h,v} = 1 - R_w^{h,v}, \quad (3)$$

with use of the Hale and Querry[13] complex refractive index. The surface reflectivity is calculated either from the Fresnel equations[1] for a smooth water surface or from the Fresnel equations applied to a random collection of specular wave facets for a wind-roughened water surface.[14] All the above steps are performed for each of the desired spectral increments.

4. Comparison of Measured and Calculated Polarization

To compare measured and calculated polarization, the polarimetric radiative transfer program was run for a smooth water surface separated from the sensor by a 1-m-long path through a 1976 U.S. Standard Atmosphere[12] (the minimum path length allowed by MODTRAN3). The reflected background path was modeled with radiosonde profiles of humidity and temperature and the Mid-latitude Winter model[12] default profiles of ozone, carbon dioxide, and other minor constituents. The radiosonde profiles are from the Denver sounding at 0000 UTC, about 3 h after the water polarization measurements were made. The other default models have air temperature at the surface of 15 °C for the 1976 U.S. Standard Atmosphere and −1 °C for the Mid-latitude Winter atmosphere, both of which are within 1 °C of the average temperatures during the measurement period. Despite the nearly equal temperature profiles from the radiosonde and the Mid-latitude Winter model, it was important to use the radiosonde data because the actual relative humidity was less than 50% of the default model relative humidity. Water vapor is the most significant contributor of atmospheric emission over much of the spectral range considered here.

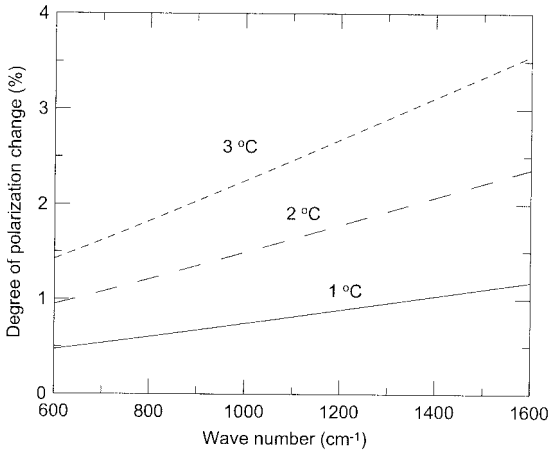

Fig. 3. Slope is introduced into the degree of polarization spectrum when the target temperature changes between acquisition of horizontally and vertically polarized spectra. Each curve is for an unpolarized target that cools by the noted amount from 40 °C.

Before a valid comparison could be made, the polarization measurements had to be corrected to remove an unusual slope that artificially elevated the high-wave-number side of the spectra. The source of this problem was identified as cooling of the water during the measurement sequence. Because this was discovered in postexperiment data processing, the experimental procedure could not be altered to minimize the problem, but a correction was derived from measurements of water at normal incidence compared with measurements of an unpolarized blackbody.

During the water polarization measurements, the water was stirred before each measurement sequence to break up the water cool skin, but during 2 h of measurements the bulk water temperature cooled from 47 °C to 32 °C. Figure 3 shows the change in polarization calculated from Eq. (1) for an unpolarized target that has cooled by different amounts from 40 °C between measurements at the horizontal and vertical polarizer settings. Figure 3 shows that even a small amount of cooling between the acquisition of horizontally and vertically polarized spectra induces a significant slope into the polarization spectra, similar to that observed in the original FTIR data. The reason is that the cooler surface produces lower radiance at the second (vertical) polarizer setting, creating a nonzero degree of polarization even when the target is unpolarized; the slope is a consequence of the shape of the Planck function.

The measured cooling during each measurement sequence (~10 min) varied between approximately 1 °C and 8 °C, depending on the sequence length and the starting air–water temperature difference. Thus the original measured polarization spectra were corrected when I subtracted an offset given by a linear fit to calculations corresponding to Fig. 3 for the measured cooling. These corrected data were vali-

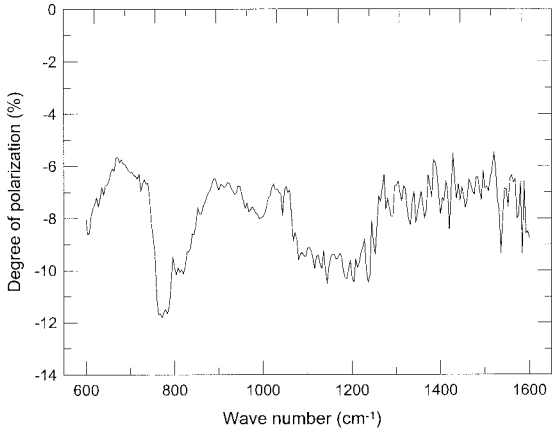

Fig. 4. Measured spectral degree of polarization for water viewed at 75° with a clear background atmosphere.

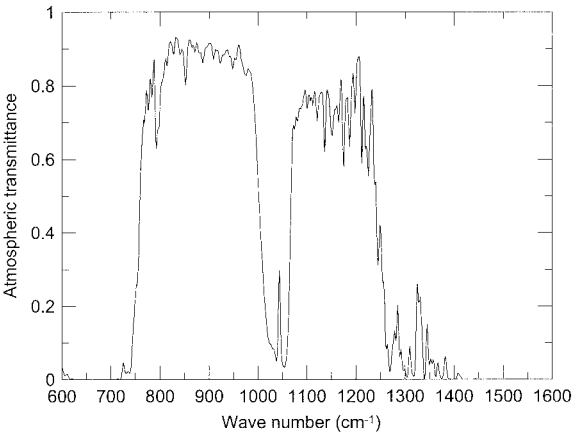

Fig. 6. Atmospheric transmittance for a 75° zenith-angle path through an atmosphere defined by local radiosonde profiles of temperature and humidity and profiles of the remaining atmospheric constituents taken from a standard Mid-latitude Winter atmosphere model.

dated in the 875–1005-cm^{-1} portion of the spectrum with measurements from a filter radiometer, which was used previously for broadband-integrated measurements of water polarization,[1] and by comparison of measurements of water at normal incidence (discussed below in this section) with measurements of an unpolarized blackbody.

Figure 4 shows the spectral degree of polarization for water measured at a 75° viewing angle over a 600–1600-cm^{-1} band with 4-cm^{-1} spectral resolution (including a slope correction as described above). Figure 5 shows the corresponding difference of measured minus calculated polarization, along with dashed lines that indicate the standard deviation of the difference across the spectrum (±0.89%). The differences are all within the measurement uncertainties of approximately 0.5% polarization in regions of high atmospheric transmissivity and 1.5% polarization in regions of low transmissivity, except for at a few particularly strong atmospheric absorption lines.

To help explain how the spectra in Figs. 4 and 5 are affected by the atmosphere, Fig. 6 shows atmospheric transmittance for a 75° zenith-angle path extending from the surface at 1.6-km elevation to space through a model atmosphere defined by radiosonde profiles of temperature and humidity, along with Mid-latitude Winter default profiles as described above. The primary absorbers are carbon dioxide (~600–700 cm^{-1}), water vapor (~700–1000 cm^{-1} and 1080–1600 cm^{-1}), and ozone (~1000–1080 cm^{-1}). The ozone absorption affects only the reflected atmospheric radiance, whereas water vapor and carbon dioxide affect both atmospheric paths. For example, note that, in the 1000–1080-cm^{-1} spectral band, ozone emission elevates the reflected background radiance, resulting in decreased net polarization. The effect of water-vapor fluctuations is especially evident in Fig. 5, explaining essentially all the larger differences. If the sensor were located even farther away from the water, the measurements would be mostly unusable at wave numbers larger than approximately 1350 cm^{-1}, especially in a humid atmosphere.

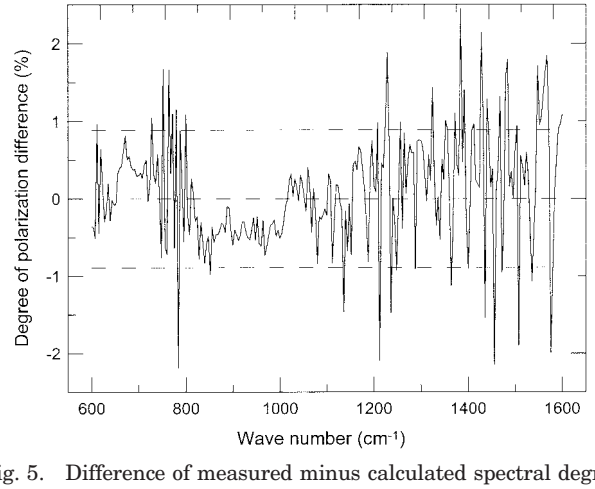

Fig. 5. Difference of measured minus calculated spectral degree of polarization for Fig. 4.

Figure 7 shows the measured polarization spectrum for water at normal incidence, also with 4-cm^{-1} spectral resolution and corrected for the above-discussed slope. At normal incidence the polarization should be zero throughout the spectrum, so any deviations are caused by measurement uncertainties or atmospheric fluctuations during the measurement sequence. The dashed lines indicate the standard deviation of this spectrum (±0.34%), and the whole spectrum could be regarded as an estimate of the spectral uncertainty in the water polarization measurements in Fig. 4. An additional measurement made with a filter radiometer (875–1005-cm^{-1} half-power bandwidth) incorporating an uncooled bolometer detector and an identical wire-grid polarizer indicated a degree of polarization of 0.00 ± 0.003 (±0.3% polarization) as the polarizer was rotated through 360°. At 75° incidence this same filter radiometer measured a band-averaged degree of polarization of −0.05 ± 0.008 (−5% polarization), which is

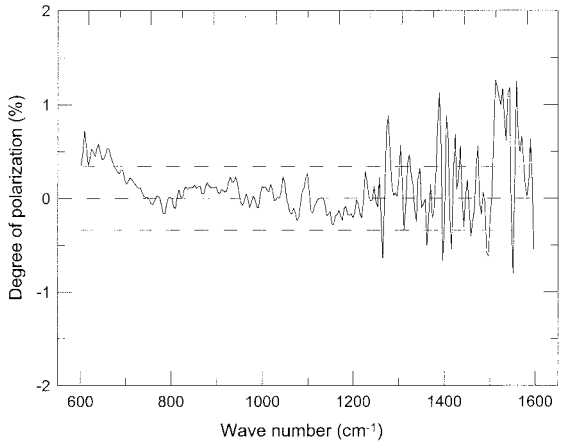

Fig. 7. Measured spectral degree of polarization for water viewed at normal incidence, for which the polarization should be zero.

less than the approximately 6.9% polarization indicated by the appropriate segment of the measured spectrum in Fig. 4, but which is within reasonable agreement when the uncertainties of both measurements are considered. This band-averaged measurement was made after all the spectral measurements were completed, so the cooler water also contributed to the lower net polarization.

5. Discussion and Conclusions

The measurements reported here provide excellent validation of the previously reported water polarization model[1] at 75° incidence, especially in the spectral regions of highest atmospheric transmittance. More careful atmospheric modeling is probably not necessary to improve the validation in spectral regions containing stronger atmospheric absorption because the atmosphere will obscure any practical measurements made in those bands. These results are the best validation yet to my knowledge of the spectral polarization signature of water in the long-wave thermal infrared spectral region. Polarization spectra at other viewing angles are similar, but with less net polarization.[1] At a viewing angle of 45° the polarization in this spectral region typically is less than 2% and reduces rapidly at smaller angles. Above 75° the polarization for a smooth surface typically becomes less than what is shown here because the reflected atmospheric radiance begins to dominate the decreasing surface emission; however, the maximum polarization can occur at angles larger than 75° for a wind-roughened surface.[1]

Validation is still needed for the shortwave region (wave numbers greater than approximately 2000 cm^{-1}), for which characterization of atmospheric aerosols and other scatterers will probably become important. Additional measurements are desirable throughout the spectrum to validate the effects of different kinds of clouds, varying atmospheric humidity, Sun and Moon glints, and varying surface roughness. Measurements made outside of spectral polarization, wind speed, and water-surface roughness would be valuable for the assessment of the effects of surface roughness. Future validation measurements would also benefit from simultaneous spectral measurements in both polarization states.

References

1. J. A. Shaw, "Degree of linear polarization in spectral radiances from water-viewing infrared radiometers," Appl. Opt. **38,** 3157–3165 (1999).
2. W. G. Egan, *Photometry and Polarization in Remote Sensing* (Elsevier, New York, 1985), pp. 337–354.
3. R. A. Millikan, "A study of the polarization of the light emitted by incandescent solid and liquid surfaces," Phys. Rev. **3,** 81–99, 177–192 (1895).
4. O. Sandus, "A review of emission polarization," Appl. Opt. **4,** 1634–1642 (1965).
5. R. D. Tooley, "Man-made target detection using infrared polarization," in *Polarization Considerations for Optical Systems II*, R. A. Chipman, ed., Proc. SPIE **1166,** 52–58 (1989).
6. T. J. Rogne, F. G. Smith, and J. E. Rice, "Passive target detection using polarized components of infrared signatures," in *Polarimetry: Radar, Infrared, Visible, Ultraviolet, and X-Ray*, R. A. Chipman and J. W. Morris, eds., Proc. SPIE **1317,** 242–251 (1990).
7. A. W. Cooper, W. J. Lentz, and P. L. Walker, "Infrared polarization ship images and contrast in the MAPTIP experiment," in *Image Propagation through the Atmosphere*, C. Daontg and L. R. Bissonnette, eds., Proc. SPIE **2828,** 85–96 (1996).
8. Y. Han, J. A. Shaw, J. H. Churnside, P. D. Brown, and S. A. Clough, "Infrared spectral radiance measurements in the tropical Pacific atmosphere," J. Geophys. Res. **102,** 4353–4356 (1997).
9. J. A. Shaw, H. M. Zorn, J. J. Bates, and J. H. Churnside, "Observations of downwelling infrared spectral radiance at Mauna Loa, Hawaii during the 1997–1998 ENSO event," Geophys. Res. Lett. **26,** 1727–1730 (1999).
10. J. A. Shaw, "The effect of instrument polarization sensitivity on sea-surface remote sensing with infrared spectroradiometers," J. Atmos. Oceanic Technol. (to be published).
11. A. Berk, L. S. Bernstein, and D. C. Robertson, "MODTRAN: a moderate resolution model for LOWTRAN7," Tech. Rep. GL-TR-89-0122 (U.S. Air Force Geophysics Laboratory, Hanscom Air Force Base, Mass., 1989).
12. G. P. Anderson, S. A. Clough, F. X. Kneizys, J. H. Chetwynd, and E. P. Shettle, "AFGL atmospheric constituent profiles (0–120 km)," Tech. Rep. AFGL-TR-86-0110 (U.S. Air Force Geophysics Laboratory, Hanscom Air Force Base, Mass., 1986).
13. G. M. Hale and M. R. Querry, "Optical constants of water in the 200-nm to 200-μm wavelength region," Appl. Opt. **12,** 555–563 (1973).
14. J. A. Shaw and C. Marston, "Polarimetric infrared emissivity for a rough sea surface," Opt. Exp. **7,** 375–380 (2000).
15. C. Cox and W. Munk, "Measurement of the roughness of the sea surface from photographs of the sun's glitter," J. Opt. Soc. Am. **44,** 838–850 (1954).
16. J. A. Shaw and J. H. Churnside, "Scanning-laser glint measurements of sea-surface slope statistics," Appl. Opt. **36,** 4202–4213 (1997).